

# DyLoRa: Towards Energy Efficient Dynamic LoRa Transmission Control

Yinghui Li, Jing Yang and Jiliang Wang

School of Software and BNRist

Tsinghua University, P.R. China

{liy16,jing-yan18}@mails.tsinghua.edu.cn, jiliangwang@tsinghua.edu.cn

**Abstract**—LoRa has been shown as a promising platform for connecting large scale of Internet of Things (IoT) devices, by providing low-power long-range communication with a low data rate. LoRa has different transmission parameters (e.g., transmission power and spreading factor) to tradeoff noise resilience, transmission range and energy consumption for different environments. Thus, adjusting those parameters is essential for LoRa performance. Existing approaches are mainly threshold based and fail to achieve optimal energy efficiency. We propose DyLoRa, a dynamic LoRa transmission control system to improve energy efficiency. The high level idea of DyLoRa is to adjust parameters to different environments. The main challenge is that LoRa has very limited data rate and sparse data, making it very time- and energy-consuming to obtain physical link properties. We show that symbol error rate is highly related to the Signal-Noise Ratio (SNR) and derive the model to characterize this. We further derive energy efficiency model based on the symbol error model. DyLoRa can adjust parameters for optimal energy efficiency from sparse LoRa packets. We implement DyLoRa based on LoRaWAN 1.0.2 with SX1276 LoRa node and SX1301 LoRa gateway and evaluate its performance in real networks. The evaluation results show that DyLoRa improves the energy efficiency by 41.2% on average compared with the state-of-the-art LoRaWAN ADR.

## I. INTRODUCTION

As an important communication platform for Internet of Things (IoT), LoRa has attracted increasing attention from both industry and academia. Being one of the representative Low Power Wide Area Network (LPWAN) techniques, LoRa is able to provide low-power long-range communication with a relatively low data rate. It is proposed to provide ultra long time communication (e.g., up to ten years) for connecting large scale of Internet of Things (IoT) devices.

The fundamental advantage of LoRa is its low-power long-range communication to achieve a very long life time. In practice, the performance of LoRa is highly related to the deployment environments [10]. The performance in terms of energy consumption, transmission distance and delay varies in different environments. Accordingly, LoRa has different parameters such as transmission power and spreading factor (SF) to tradeoff transmission energy consumption, noise resilience and transmission range to adapt to different environments. For example, increasing transmission power and spreading factor would make the transmission more resilient to noise and increase the transmission range, while on the other hand increase the energy consumption. Moreover, LoRa have relatively long packet transmission time and high transmission

cost, e.g., with the largest SF and transmission power, a packet of 100 bytes can take 2184.6 ms to transmit and cost 959 mJ energy. Adjusting those parameters would significantly impact the performance. Therefore, carefully setting the parameters for each packet in real LoRa deployment is very important for LoRa energy efficiency.

Existing transmission control approaches to set parameters in LoRa are mainly threshold based and can hardly achieve optimal energy efficiency. The state-of-the-art approach, Adaptive Data Rate control (ADR) [21], selects the minimal SF and transmission power while keeping the SNR above the demodulation floor. Considering the energy efficiency as the number of delivered bits per unit of power consumption, we show that there exists a huge gap between the energy efficiency of state-of-the-art transmission control approach ADR and the optimal solution. Our experiment shows that ADR may result in up to 103% more energy consumption. This leads to significant unnecessary energy waste especially for the very resource constrained LoRa nodes which are supposed to work for years.

Dynamic transmission control and parameter adjustment has been studied in many research works like in wireless sensor networks [14], [22], [27], [30], WiFi [24], etc. Those approaches achieve very good performance in transmission control and can search for optimal transmission parameters to improve reliability, delay and power consumption. Those approaches, however, cannot be directly applied to LoRa networks. LoRa provides ultra low data rate and low power communication. It usually works in a very low duty cycle mode and the traffic in LoRa may be very sporadic. Considering the relatively long packet time and low duty cycle, it is usually very time consuming to obtain the common link statistical properties. It takes a long time to evaluate the performance of different parameter settings or obtain performance statistics. Therefore, the limited information available from LoRa transmission and high overhead to obtain information hinder the direct application of existing dynamic control approaches.

We propose DyLoRa, a dynamic LoRa transmission control system to improve energy efficiency for LoRa in different environments. The high level idea of DyLoRa is to set the optimal parameters based on the physical LoRa link properties. We derive a model to characterize energy efficiency based on transmission parameters by leveraging LoRa link properties. More specifically, according to the mechanism of LoRa

demodulation, our model can characterize the Symbol Error Rate (SER) from Signal-to-Noise Ratio (SNR) and transmission parameters. Then, given the LoRa coding scheme, the model characterizes Packet Delivery Ratio (PDR) and the energy efficiency based on the symbol error. Based on the model, we can finally derive the optimal parameter settings upon each packet reception. DyLoRa can derive parameter settings for optimal energy efficiency with very limited packets. This enables DyLoRa applicable to the low data rate LoRa with sparse traffic.

We implement DyLoRa based on LoRaWAN 1.0.2 with LoRa node based on SX1276 and gateway based on SX1301. In practice, we find that the model for energy efficiency may vary according to different hardware implementation. Thus we adapt the model to practical hardware configuration with received packets. We validate our model and show that it can effectively and accurately derive the packet error rate and thus PDR upon each packet reception. We evaluate the performance of our system in both indoor and outdoor environments. The evaluation results show that DyLoRa is able to improve the energy efficiency by 41.2% on average.

Our contributions are summarized as follows.

- We show the energy efficiency gap between the state-of-the-art transmission control method and the optimal solution. We propose DyLoRa, a LoRa transmission control system to optimize energy efficiency.
- We propose a model to characterize energy efficiency for LoRa transmission based on transmission parameters such as transmission power, spreading factor, and SNR. Based on the model, we derive optimal transmission parameter settings to adapt to different environments.
- We implement DyLoRa based on LoRaWAN 1.0.2 with LoRa node based on SX1276 and gateway based on SX1301. We evaluate DyLoRa in real networks and the results show that DyLoRa improves the energy efficiency by 41.2% on average.

The paper is organized as follows. Section II introduces basic knowledge of LoRa and LoRaWAN. Section III states our motivation and possible challenges in detail. Section IV describes the system design and implementation. Section V evaluates the proposed algorithm. Section VI introduces related works. Finally, section VII concludes the work.

## II. LORA BACKGROUND

In this section, we present a basic introduction of LoRa. We start with LoRa's modulation and demodulation scheme, and then we discuss how the transmission parameter settings impact the LoRa performance. We finally introduce the widely used Adaptive Data Rate (ADR) control method on LoRa.

### A. LoRa Modulation and Demodulation

LoRa employs Chirp Spreading Spectrum (CSS) modulation technique in the PHY layer. A LoRa symbol is an up-chirp signal that sweeps linearly from a start frequency  $f_0$  to the frequency  $f_0 + B$ , where  $B$  is the bandwidth. Therefore, a chirp in the baseband can be denoted as  $c(t) = e^{2\pi(f_0 + \frac{B}{2T}t)t}$ ,

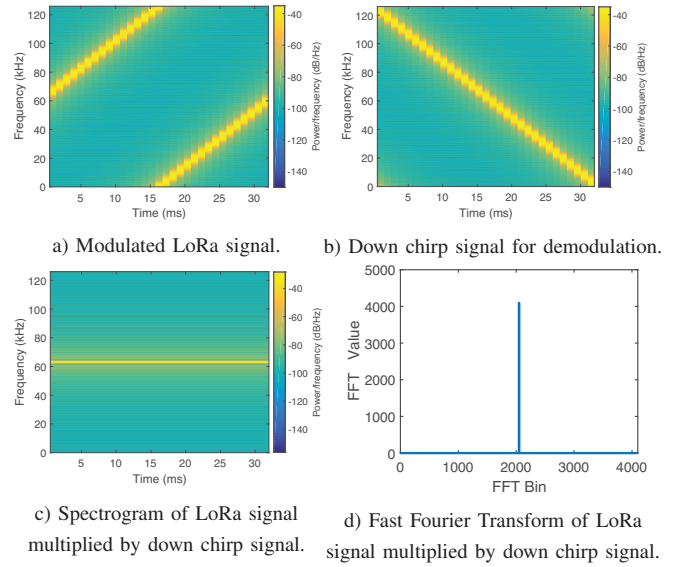


Fig. 1: LoRa demodulation procedure. Figure a shows the spectrogram of LoRa signal. Figure b shows the spectrogram of down chirp signal. When the gateway receives a LoRa signal, it multiplies the LoRa signal with a down chirp signal. The spectrogram of the product is shown in Figure c. Then the gateway applies fast fourier transform (FFT) on the product, and chooses the frequency of the FFT peak to calculate the symbol. Figure d shows the FFT result.

where  $T$  is the duration of the chirp. The frequency of a chirp is constrained in bandwidth  $B$ , i.e., the frequency larger than  $B$  will be aliased down to  $((f_0 + B) \bmod B)$ . LoRa modulates the transmitted data in the start frequency  $f_0$ .

Figure 1 shows the demodulation procedure. When a LoRa signal is detected, the receiver decodes the signal [19] as follows:

- Emulate a base-band down-chirp signal (Figure 1 b) of which the frequency decreases linearly from the bandwidth to zero.
- Multiply the received signal by the emulated down-chirp signal, the product is of a constant frequency, as shown in Figure 1 c. In fact, the constant frequency is equal to the start frequency of the LoRa signal.
- Apply Fast Fourier Transform (FFT) on the multiplied signal.
- Find the highest peak of the FFT result, as shown in Figure 1 d. The frequency of the highest peak indicates the modulated data.

The modulation and demodulation scheme enable LoRa to achieve a long distance and low data rate transmission of LoRa even under a low SNR.

### B. Impact of Spreading Factor and Transmission Power

There are multiple parameters in LoRa that significantly impact the LoRa performance. In order to adapt to different environments, e.g., transmission distance, LoRa adopts Spreading Factor (SF) to adjust the resistance to noise by changing the chirp duration. In LoRa, the value of SF ranges

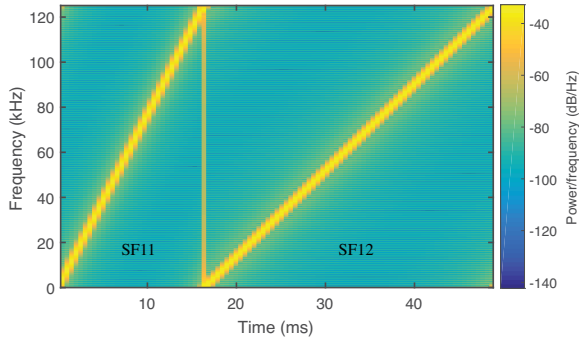


Fig. 2: The symbol durations are different under different SFs.

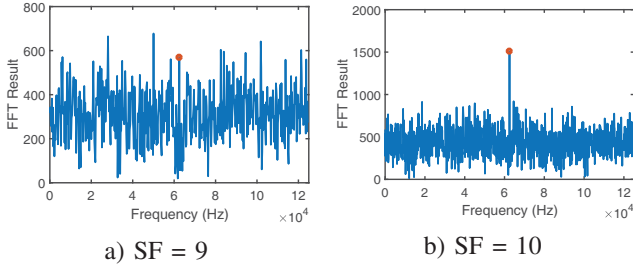


Fig. 3: The blue line indicates the Fast Fourier Transform result of all frequencies. The red circle indicates the FFT result of the target frequency. LoRa packet is more resilient to noise with larger SF under the same noise level. Figure a shows when SF=9, the FFT result of at the target frequency is not strongest, so the symbol will not be correctly decoded. Figure b shows when SF = 10, the signal's FFT result at the target frequency is the largest, and the symbol will be successfully decoded.

from 7 to 12. The duration of a chirp is proportional to  $2^{SF}$ , as shown in Fig. 2. Meanwhile, the number of bits modulated per chirp is equal to SF. The relation between the chirp length  $T$  and SF can be denoted as

$$T = \frac{2^{SF}}{B} \quad (1)$$

When the SF is increased by 1, the duration of a chirp is doubled. Fig. 2 shows chirps of SF = 11 and SF = 12 respectively.

Thus, the data rate  $DR$  can be calculated as

$$DR = \frac{SF \cdot B}{2^{SF}} \quad (2)$$

We can see that on one hand increasing SF reduces the data rate. On the other hand, it will increase the link budget and make the signal more resilient to noise. Fig 3 explains why increasing SF improves the symbol's resilience to noise. Larger SF means longer symbol duration. The FFT value of the signal increases along with the symbols duration, while the FFT result of noise remains almost the same. Thus, the receiver is able to decode the signal with larger SF. Increasing SF improves the resistance to noise, and further leads to increasing on transmission distance.

Increasing transmission power (TP) will improve the signal

strength, while incurring more energy consumption. LoRa defines 8 transmission power levels from 0 to 7. The transmission power of each level is related to the hardware implementation. We measured the transmission power of our end nodes and the results are shown in Tab. II. The measurement procedure is detailed in Section V.

### C. Adaptive Data Rate Control in LoRa

To adapt to different environments, the widely used LoRa protocol LoRaWAN [2] integrates Adaptive Data Rate (ADR) control [23]. The ADR enables LoRa to set appropriate TP and SF for end nodes.

In LoRaWAN, the ADR control utilizes a threshold based method to choose the SF and TP [21]. The ADR algorithm maintains an SNR floor of each SF, which enables the gateway to successfully demodulate LoRa symbols of each SF. It estimates SNR from recent packets, and choose the minimal SF that results in SNR above the corresponding SNR floor. The transmission power is set to maximum by default. The only case to adjust transmission power is when the SF is set to minimal and the SNR is still higher than the SNR floor. The algorithm will try to decrease the transmission power before the SNR reaches the SNR floor. The ADR control runs on the gateway and the SF and transmission power parameters are sent to the end node.

## III. MOTIVATION

LoRa is supposed to provide ultra low power transmission and long time (up to ten years) communication. However, in this section, we show the energy efficiency in current LoRa design is still far from efficient even with ADR. We explore the impact of transmission power and SF on energy efficiency. We present the motivation and challenges on optimizing the energy efficiency.

We measure the energy consumption for LoRa under ADR as well as different transmission power (TP) and SF settings. The LoRa node in our experiment is based on SX1276 chip and our gateway is based on SX1301 chip. As in usual application, the gateway is placed on the roof of a office building. The node is placed 1200 m away from the gateway. We choose different combinations of SF (7-12) and TP (205 mw - 439 mw) settings. In each setting, we transmit 100 packets with 45 bytes payload, and calculate the energy efficiency and PDR in each setting. The energy efficiency is calculated by the average number of bits transmitted given a certain amount of energy.

Fig. 4 (a) shows the impact of transmission power when SF is fixed to 8. The energy efficiency fluctuates under different transmission power. The energy efficiency first increases and then drops as the transmission power further increases. This is reasonable. When the TP increases at the beginning, the PDR increases due to increase in SNR and the number of successfully transmitted bits also increases. Thus the energy efficiency increases. However, further increase on TP brings marginal benefit on SNR and PDR. We can see that there is a gap between the current achieved energy efficiency (ADR) and the optimal energy efficiency. This also tells us selecting

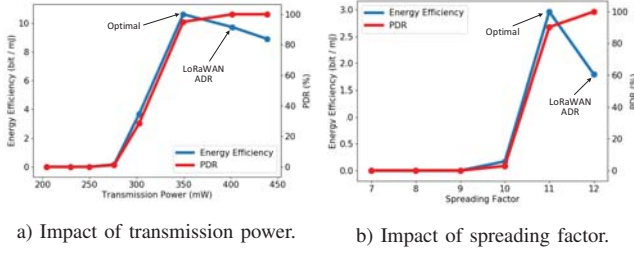


Fig. 4: The transmission power and spreading factor impact the packet delivery rate and energy efficiency. Figure a shows the impact of transmission power on energy efficiency and the transmission power selection results. Figure b shows the impact of spreading factor and the selection results. LoRaWAN ADR results in suboptimal energy efficiency choice.

the highest PDR (as in ADR) does not always lead to best energy efficiency.

Then we fix TP to 205 mW and evaluate the impact of SF. Fig. 4 (b) shows that the impact of SF to energy efficiency and PDR. First, we can see that increasing on SF first increases the energy efficiency and then decreases the energy efficiency. This is because increasing SF on one hand increases PDR and on the other hand also increases the time length of each packet. Second, we can also see a gap for energy efficiency between existing ADR and the optimal energy efficiency. The optimal energy efficiency is about 40% higher than that of ADR. We observe that the ADR algorithm choose the setting that guarantees the best PDR in figure 4. The ADR claims to choose the smallest SF and transmission power that the SNR is above the corresponding SNR floor. However, the result shows that the ADR tends to select larger SF and TP. This is because that the ADR chooses conservative SNR floors to guarantee the PDR performance.

Therefore, we need to dynamically select the transmission parameter in order to achieve optimal energy efficiency. Dynamic packet transmission control is not new in wireless transmission. However, when it comes to LoRa, there are new challenges that we need to address before make it applicable to real applications.

A possible way is to let each LoRa node test every combination of TP and SF settings. Each node measures the energy efficiency of each combination of settings and then chooses the best one. The problem is that traversing all the settings takes a long time. There are  $6 \times 8 = 48$  different combinations of transmission power and spreading factor. Assuming a LoRa node sends 100 packets to measure the energy efficiency in each setting, and the time interval is 15 seconds between two packets, it takes 20 hours to complete the measurement for each setting. In practice, the data traffic in LPWAN application is even more sporadic which makes it even longer for each measurement. Moreover, the link quality may change over time. The best settings needs to be updated from time to time.

**Summary.** There exists a gap between the energy efficiency of ADR and the real achievable optimal energy efficiency. Filling this gap would significantly reduces the energy con-

sumption of existing LoRa and prolong its life time. It is also challenging to achieve optimal energy efficiency in LoRa network with a low data rate.

#### IV. DYLoRA DESIGN

##### A. Design Overview

**Goal.** Denote EE, TP, DR and PDR as energy efficiency, transmission power, data rate and packet delivery rate, the energy efficiency can be calculated as

$$EE(TP, SF) = \frac{DR(SF) \times PDR(TP, SF)}{TP} \quad (3)$$

The system goal is to select the parameters, i.e., transmission power (TP) and spreading factor (SF), to maximize the energy efficiency.

**Challenges.** Usually, this can be achieved if we know the PDR and DR under different combinations of parameters. However, LoRa is proposed to support ultra low data rate and low power communication. Meanwhile, LoRa usually works in a very low duty cycle mode and the traffic in LoRa is very sporadic. Unlike dynamic transmission control methods in traditional networks, it is usually very energy and time consuming to obtain the statistical results for PDR and DR. Therefore, the challenge is how to dynamically adapt to the optimal parameters with low data rate. Moreover, the relationship between energy efficiency and transmission parameters varies under different hardware and environments. The proposed approach should adapt to different hardware settings and environments.

**Main Design.** We propose DyLoRa, a dynamic LoRa transmission control system to optimize energy efficiency with information derived from each received packet, to adapt to LoRa network with sparse traffic. The high level idea of DyLoRa is to leverage the physical properties of LoRa transmission. According to the mechanism of LoRa demodulation, we show that the demodulation symbol error rate is highly related to the SNR and thus derive the model to characterize symbol error rate. Further, we propose a method to estimate packet error based on the symbol error model. In practice, we find that due to hardware implementation diversity, the model varies in different hardware platforms. We adapt our packet error model to practical hardware configuration with information extracted from packets. We validate our model and show that it can effectively and accurately derive the packet error rate and thus energy efficiency with a small number of packets. This is very important for dynamic LoRa transmission control especially for a network with relative sparse traffic.

The DyLoRa system architecture is shown in Fig. 5. DyLoRa includes two parts: DyLoRa Gateway and DyLoRa Node. DyLoRa Gateway tracks the end node's link quality and controls the node's spreading factor and transmission power. DyLoRa Node monitors the node's connectivity to the gateway, and recovers the connection when the node is offline. DyLoRa Gateway runs at the gateway. When a packet arrives, DyLoRa Gateway extracts the average SNR of recent  $n$  packets as an indicator of link quality, where



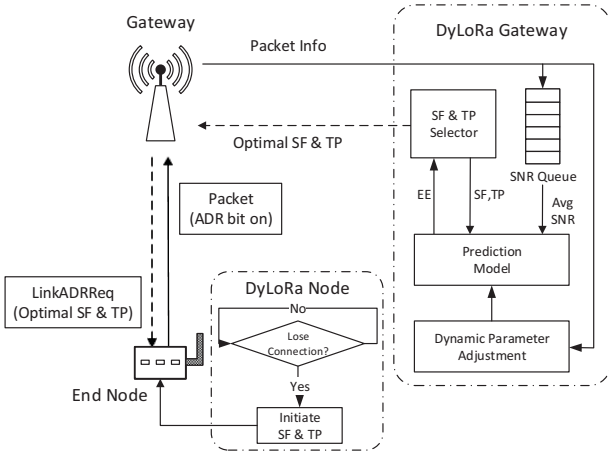


Fig. 5: System Architecture of DyLoRa

$n$  is a pre-defined value and in this paper we set  $n$  as 6. Then DyLoRa Gateway traverses all the SFs and TPs. Each combination of SF and TP is input into the prediction model along with the average SNR. The prediction model calculates the estimated energy efficiency and returns it to DyLoRa Gateway. DyLoRa Gateway compares the energy efficiencies of all the SF and TP settings, and selects the most energy efficient spreading factor and transmission power. Then the selected parameters are sent to the end node. Meanwhile, DyLoRa gateway periodically adjusts the parameter setting of prediction model. The basic idea is to adjust the parameters to reduce the difference between the prediction result and the measured energy efficiency.

DyLoRa Node runs at the end node. When the end node receives the setting of spreading factor and transmission power, it changes the transmission settings accordingly. Meanwhile, DyLoRa Node continuously monitors the node's connectivity to the gateways. If the number of lost down-link packets exceeds a threshold  $\delta$ , DyLoRa Node resets the spreading factor and transmission power to maximum to ensure the connectivity to gateway.

### B. Prediction Model

In the DyLoRa gateway, the first task is to estimate the parameters used for optimizing the energy efficiency EE. To solve the problem, we propose a model to calculate the energy efficiency under different spreading factor and transmission power. The energy efficiency can be calculate via DR, PDR and TP as shown in Eq. 3. We discuss those three parameters separately.

1) *Data Rate*: The data rate is the amount of data transmitted per second. Given the spreading factor SF, the data rate can be calculated based on the SF and bandwidth  $B$  as shown in Eq. 2, where  $B$  can be obtained from the packet.

2) *Transmission Power*: LoRa defines 8 different transmission power levels corresponding to different signal gain. The



Fig. 6: LoRa PHY Packet Format

exact transmission powers and the signal gains of each level can be derived by measurement.

We measure the transmission power and signal gain of our end nodes. We use the power monitor [1] to measure the power consumption rate of each power level. The measurement is carried out only once for our system.

3) *PDR*: A LoRa packet is composed of a sequence of chirp symbols. Meanwhile, LoRa uses forward error coding to improve the packet delivery rate. We first consider the symbol error rate, and then model the packet delivery rate.

Before modeling the symbol error rate, we briefly recall the LoRa demodulation procedure. When a signal is detected, the receiver multiplies the received signal by a down chirp signal. The demodulation procedure aggregates the signal energy  $E_S$  to a single frequency. Meanwhile, the noise energy  $E_N$  is distributed among different frequencies. The signal is decoded successfully as long as the signal energy exceeds the noise energy. The bandwidth is divided into  $2^{SF}$  channels and the noise energy in each channel is  $E_i$ ,  $i = 1, 2, \dots, 2^{SF}$ . Assuming the symbols is modulated in channel  $j$ , The symbol error rate  $P_b$  is calculated as

$$P_b = 1 - P(E_S + E_j > \max_{i \neq j} E_i) \quad (4)$$

As  $SNR = 10 \log_{10}(E_S/E_N)$ , and  $E_N = \sum_{i=1}^{2^{SF}} E_i$ , Eq. 4 is equal to

$$P_b = 1 - P(10^{SNR/10} \sum_{i=1}^{2^{SF}} E_i + E_j > \max_{i \neq j} E_i) \quad (5)$$

Modeling the link as an AWGN channel,  $P_b$  can be calculated [16] as

$$P_b(SNR, SF) = 0.5 \times Q(\sqrt{10^{SNR/10} \times 2^{SF+1}} - \sqrt{1.386 \times SF + 1.154}) \quad (6)$$

where  $Q(\cdot)$  is the tail function of the standard normal distribution.

Before modeling the packet delivery rate, we briefly introduce the impact of packet format and error correction mechanism of each part.

The physical uplink message format is shown in Fig 6. The packet contains three components: preamble, physical header and the payload. The preamble contains a sequence of  $(n+2)$  up-chirps, 2 down-chirps and 0.25 up-chirp. The total length of the preamble is  $(n + 4.25)$ , where  $n$  is a user-defined value. Both header and payload employ the forward error coding. The coding rate of header is set to 4/8 and the coding rate of payload is set to 4/5 by default.

The preamble detection procedure is different from LoRa demodulation. It correlates the received signal with the ideal

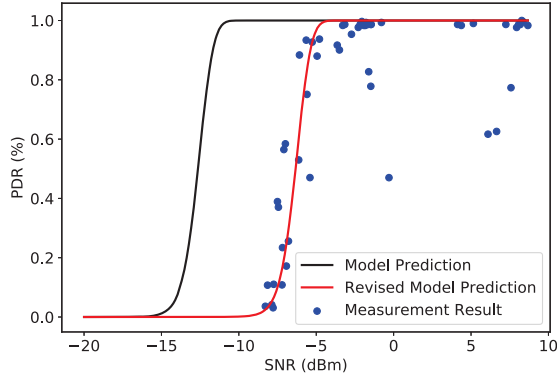


Fig. 7: PDR Gap between model predictions and measurement results. SF = 7.

preamble chirps [11]. If the correlation is above a predefined threshold, a preamble is successfully detected. Correlation with an ideal chirp has the same gain as the LoRa demodulation, and thus the same detection probability. Consider the preamble as a LoRa symbol modulated with spreading factor  $SF + \log_2(n + 4.25)$ . Thus, we can utilize Eq. 6 to model the preamble detection probability as

$$P_{preamble} = P_b(SNR, SF + \log_2(n + 4.25)) \quad (7)$$

LoRa uses Hamming code for forward error correction. The header has a fixed 4/8 coding rate, i.e., 4 redundant bits are added per 4 data bits. The 4 redundant bits can at most correct 1 bit error. Therefore, the 4 bits can be correctly decoded when there is at most 1 bit error. Assuming the length of header is  $L_h$ , the header decoding probability  $P_h$  is

$$P_h(SNR, SF) = ((1 - P_b)^4 + 3(1 - P_b)^7 P_b)^{\lceil L_h/4SF \rceil} \quad (8)$$

The coding rate of the payload depends on the transmission settings. Let CR = 1 to 4 denote coding rate of 4/5, 4/6, 4/7 and 4/8, respectively. It should be noted that coding rate 4/5 and 4/6 cannot correct the bit error but only detect error, while coding rate 4/7 and 4/8 can correct 1 bit error of 4 bits. So, different coding rate has different decoding probability. Denote the number of payload bits as  $L_p$ , we can calculate the probability of decoding payload as

$$P_p(SNR, SF) = \begin{cases} (1 - P_b)^{\lceil \frac{L_p}{SF} \rceil}, & CR = 1, 2 \\ ((1 - P_b)^4 + 3(1 - P_b)^7 P_b)^{\lceil \frac{L_p}{4SF} \rceil}, & CR = 3, 4 \end{cases} \quad (9)$$

Then the PDR of the packet can be calculated as

$$PDR(SNR, SF) = P_{preamble} \times P_h \times P_p \quad (10)$$

The transmission power impacts the SNR. Given a transmission power, it is challenging to derive the SNR as the environment is unknown. However, we show that given the SNR under a certain transmission power, we can derive the SNR under other different transmission power. We can lever-

age the SNR gain of different transmission power as listed in Table II. The SNR gain indicates the SNR difference between two different transmission power levels. Denote current SNR and transmission power as  $SNR'$  and  $TP'$ , the packet delivery rate can be calculated as

$$PDR(TP, SF) = PDR(SNR' + Gain(TP', TP), SF) \quad (11)$$

Function  $Gain(TP', TP)$  calculates the SNR difference between  $TP'$  and  $TP$  by looking up Table II.  $SNR'$  and  $TP'$  are derived from the received packet.

As a summary, the prediction model takes SF, TP and SNR as inputs, and outputs estimated energy efficiency. To achieve this, the prediction model first calculate data rate DR via Eq.2, and then calculate the PDR via Eq.11. Finally, the prediction model gets energy efficiency with Eq.3.

### C. Dynamic Parameter Setting with Prediction Model

In practice, the real network performance deviates from the theoretical model. We collect data from our testbed to examine the difference between the model prediction and the ground truth.

We can see a difference between the model and real performance as shown in Fig. 7. The black line shows the prediction of the model, and the blue dots are the measured results from real data. We can see that there is a huge gap between the model prediction and real performance. Thus, it is essential to bridge such gap before using the model for SF and TP selection. We solve the problem by adding a dynamic offset on SNR in Eq. 11, i.e.

$$PDR(SNR, SF) = PDR(SNR' + Gain(TP', TP) + offset(SF), SF) \quad (12)$$

where  $offset(SF)$  denotes the SNR offset of SF. The offset is derived by calculating the SNR difference between model prediction and measurement result. Table I presents the SNR offset in our testbed. As shown in Fig. 7, the red line shows the prediction of the adapted model. It shows that the adapted model fits the real measurement results well. Thus, in DyLoRa, we use Eq. 12 instead of Eq. 11 for energy efficiency prediction. DyLoRa dynamically shifts the SNR offset to fit the estimated energy efficiency to approach the real performance.

We formally describe the transmission control algorithm of DyLoRa in Algorithm 1. Lines 1-3 declare the inputs of the algorithm. Line 5 calculates the average SNR  $snr_{stack}$  of historical packets. Lines 6-15 take all combinations of TP and SF, and calculate the energy efficiency of each combination. Then the selected setting of SF and TP is sent to the end node via *LinkADRReq* command. Lines 17-25 detail how to calculate the energy efficiency given the SF, TP and the packet information according to Eq. (6-11).

TABLE I: SNR Gain and Power under Different Power Level

SF	7	8	9	10	11	12
SNR offset (dBm)	-6.3	-6.5	-6.8	-7.3	-8	-9.5

---

**Algorithm 1** SF & TP Selection Algorithm

---

```

1:  $snr$ : packet snr;  $tp_{list}$ : power level 0 to 7
2:  $sf_{list}$ : sf7 to sf12;  $bw$ : bandwidth;  $cr$ : coding rate
3:  $n_p$ : preamble length;  $L_h$ : header length;  $L_p$ : payload length
4:
5:  $snr_{es} = Average(snr_{stack})$ 
6: for  $tp, sf$  in  $tp_{list}, sf_{list}$  do
7:    $ee = GetEE(sf, snr_{es}, cr, n_p, L_h, L_p)$ 
8:   if  $ee$  is optimal then
9:      $Return(sf, tp)$ 
10:  end if
11: end for
12:
13: Function  $GetEE(sf, snr_{es}, cr, n_p, L_h, L_p)$ 
14:  $br = sf \times bw / 2^{sf}$ 
15:  $snr = snr_{es} + Gain(tp)$ 
16:  $\Gamma = 10^{(snr + offset(sf))/10}$ 
17:  $P_b = 0.5 \times Q(\sqrt{\Gamma \times 2^{sf+1}} - \sqrt{1.386 \times sf + 1.154})$ 
18:  $P_h = ((1 - P_b)^4 + 3(1 - P_b)^7 P_b)^{\lceil L_h / 2SF \rceil}$ 
19: if CR equals 1 or 2 then
20:    $P_p = (1 - P_b)^{\lceil L_h / SF \rceil}$ 
21: else
22:    $P_p = ((1 - P_b)^4 + 3(1 - P_b)^3 + CR P_b)^{\lceil L_h / 4SF \rceil}$ 
23: end if
24:  $sf' = sf + \log_2(n_p)$ 
25:  $P_{pre} = 0.5 \times Q(\sqrt{\Gamma \times 2^{sf'+1}} - \sqrt{1.386 \times sf' + 1.154})$ 
26:  $pdr = P_{pre} \times P_{header} \times P_{payload}$ 
27:  $ee = dr \times pdr / tp$ 
28: Return  $ee$ 

```

---

## V. EVALUATION

We evaluate DyLoRa in this section. We first evaluate the performance of energy efficiency model, then compare DyLoRa with ADR algorithm in LoRaWAN [21].

### A. Implementation & Experiment Settings

We implement DyLoRa based on LoRaWAN 1.0.2. The LoRa node used in our implementation is based on SX1276 and the gateway is based on SX1301. The gateway is placed on the roof of a 4-floor building. The node and gateway run in 470-510 MHz frequency range. The bandwidth of each channel is set to 125 kHz. The payload length is set to 45 bytes and the preamble has a length of 8 bytes.

We measure the transmission powers and the signal gains of different power levels. We use the Power Monitor [1] for the transmission power measurement. At each power level, the node sends 5 packets to measure the average power consumption for transmission. We also measure the signal gain of each power level. A node is placed about 50 meters away from the gateway. At each power level, the node sends 100 packets to the gateway and we calculate the average RSSI value. We take the RSSI value of power level 7 (the minimal power level) as baseline, and calculate the RSSI difference between each power level and power level 7 as the signal gain. Tab. II shows the measurement results of transmission powers and the corresponding transmission signal gain.



Fig. 8: Deployment of nodes and the gateway

TABLE II: Transmission Power Level and Gain

Power Level	7	6	5	4	3	2	1	0
Power (mW)	205	230	250	276	303	350	402	439
Gain (dBm)	0	1.6	2.8	4	5.2	6.4	7.7	8.9

To evaluate the energy efficiency model, we collect the data of 30 outdoor nodes during 15 days. Each node sends a packet every minute or 5 minutes. We first calculate the energy efficiency, SF and average SNR of each node during each hour, and then we compare with the energy efficiency prediction results.

To compare the performance of DyLoRa with the ADR algorithm, we conduct an experiment with 11 nodes. Among these nodes, 7 nodes are outdoor nodes and 4 are indoor nodes. The deployment of the nodes and the gateway are shown in Fig. 8. Each node is initiated with SF12 and transmission power level 0. The packet interval of each node is set randomly between 15-30 seconds. We compare DyLoRa and ADR on those nodes. We evaluate the performance of DyLoRa and ADR for more than one hour. We then compare the final chosen settings and the energy efficiency performance between two approaches.

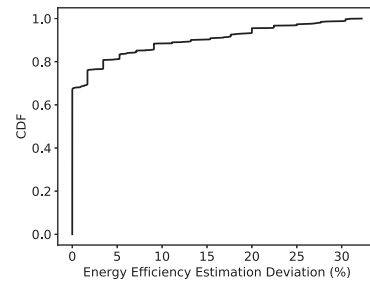


Fig. 9: Cumulative distribution of the energy efficiency estimation deviation.

### B. Energy Efficiency

We split the data into different groups. Each group is composed of data from one node within an hour. We calculate the energy efficiency of each group, along with the average

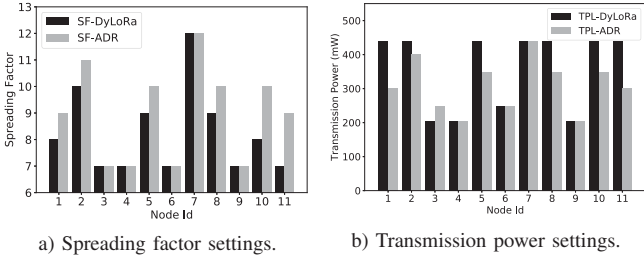


Fig. 10: Selected spreading factors and transmission power levels of the 11 nodes. Figure a shows the spreading factor settings of DyLoRa and ADR on each node. Figure b compares the transmission power settings of each node under DyLoRa and ADR.

SNR, SF and transmission power. Then we feed the SNR, SF and transmission power into our model and estimate the energy efficiency. Finally we compare the estimated energy efficiency with the measured energy efficiency. Denote the estimate and ground truth energy efficiency as  $EE_{est}$  and  $EE_{tru}$ , we take the estimation deviation,  $(EE_{est} - EE_{tru})/EE_{tru}$ , as the criteria.

The comparison result is shown in Fig. 9. The figure shows that estimation deviation is within 15% for 90% of cases. DyLoRa is able to predict the energy efficiency under various settings with a high accuracy.

### C. Comparison with ADR Algorithm

The final SF and transmission power of each node are shown in Fig. 10. We see that 4 nodes are set to the same SF and transmission power by two algorithms. This is because that the link quality is very good or very bad. Thus those two approaches would set to the same setting. However, when the link is in transitional region, there is obvious difference between the parameter settings. DyLoRa prefers to use smaller SF and higher transmission power than that of ADR.

Then we compare the energy efficiency and packet delivery rate performance of two algorithms. In figure 11a, we see that DyLoRa outperforms ADR among all nodes with transitional link quality. Figure 11b shows DyLoRa's energy improvement distribution compared with the ADR. The improvement is up to 103% at node 11, and the average energy efficiency improvement is 41.2%. Meanwhile, DyLoRa slightly sacrifices the PDR for energy efficiency. Figure 12 shows that the PDR degradation is limited. The largest PDR difference is within 15%. Such PDR performance reduction is acceptable given the energy efficiency improvement. The evaluation shows that DyLoRa can improve the energy efficiency at a limited cost of PDR.

## VI. RELATED WORK

With the fast development of LoRa, there are emerging research works exploring the performance, applicability and limitations of LoRa and LoRaWAN.

### A. LoRa Adaptive Data Rate Control

Sundaram et al. have discussed the energy consumption problem in [29]. The authors show that LoRa end-devices

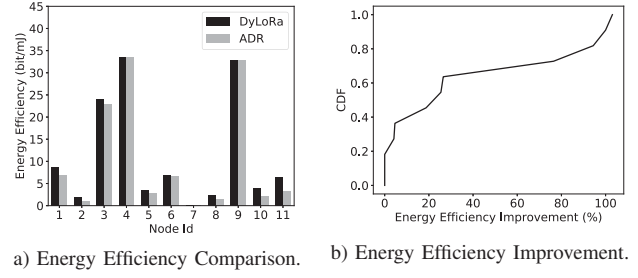


Fig. 11: Energy efficiency comparison between DyLoRa and ADR. Figure a shows the energy efficiencies of each node. Figure b shows the cumulative distribution function of DyLoRa's energy efficiency improvement compared with LoRaWAN ADR.

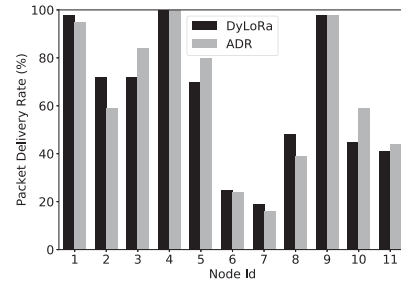


Fig. 12: Packet delivery rate comparison between the energy efficiencies of DyLoRa and ADR's parameter settings on each node.

consume more power than expected. Thus, it is important to optimize the energy efficiency. There have been a series of works on LoRa's adaptive data rate control. [3] adjusts the data rate according to the congestion status. The system contains a congestion classifier and a data rate controller. If the channel is congested, the data rate controller will change the back-off time to avoid collision. [12] focuses on optimizing the Data Extraction Rate (DER). The key observation is that the DER drops quickly when the number of end devices increases in the same channel with the same SF. The authors propose an SF allocation algorithm. The algorithm first calculate the usable SF list of each end device according to the signal's RSSI and the sensitivity of each SF, and then assign SF to each node to balance the air time of each node. Similarly, in [4] the authors also focus on optimizing the whole system's performance. The difference is that they are more focused on the transmission fairness for each node. In [21], the authors propose a SNR-based adaptive data rate algorithm. The authors estimate the SNR threshold of each SF. Then the algorithm assigns the minimal SF according to the threshold. Gao et al. focus on the energy fairness of large scale LoRa networks [18].

### B. LoRa Measurements & Applications

The works in [6] [28] [5] [8] provide a detailed introduction to LoRa network structure, LoRa modulation and demodulation scheme. The authors propose a detailed power model of LoRaWAN in [9]. [5] focuses on the limitations of LoRaWAN. [7] analyzes a mathematical model of LoRaWAN's network load considering the acknowledged uplink transmission with



class A. The authors point out that the PER grows rapidly to 1 when the load exceeds a threshold. [26] provides a thorough review on LoRa testbeds.

[25] summaries different applications based on LoRa, including temperature monitor, water level monitoring system, water grid sensing, etc. Adwait et al. presents an application architecture built on LoRaWAN [13] that simplifies the design and deployment of IoT devices. [15] utilizes the hardware difference to enable concurrent packet transmission on the same channel. Tim et al. [20] use LoRa as the communication module to improve the battery life of the GPS tracker. Bernat and Martin [17] try to use locate LoRa devices without a GPS unit. They collect the time difference when a packet arrives at multiple gateways, and implement a TDOA localization algorithm.

## VII. CONCLUSION

We propose DyLoRa, a dynamic LoRa transmission control system to optimize energy efficiency. DyLoRa aims to fill the energy efficiency gap between the state-of-the-art transmission control and the optimal solution. The high level idea of DyLoRa is to leverage the physical properties of LoRa and build a model for energy efficiency under different transmission parameters including transmission power and spreading factor. DyLoRa can derive parameter settings for optimal energy efficiency with very sparse LoRa data traffic. We implement DyLoRa on LoRaWAN 1.0.2 with SX1276 based LoRa node and SX1301 based LoRa gateway. We evaluate DyLoRa in real deployments and the evaluation shows that DyLoRa is able to improve the energy efficiency by 41.2% on average. We believe DyLoRa can be an important and effective approach to improve energy efficiency for real LoRa deployments.

## ACKNOWLEDGEMENTS

This work is in part supported by National Key R&D Program of China 2018YFB1004800, National Natural Science Fund for Excellent Young Scholars (No. 61722210), National Natural Science Foundation of China (No. 61932013, 61532012, 61632008).

## REFERENCES

- [1] Power monitor. <https://www.msoon.com/powermonitor-support>.
- [2] The things network. <https://github.com/TheThingsNetwork/ttn>.
- [3] Adaptive data rate control in low power wide area networks for long range iot services. *Journal of Computational Science*, 22:171 – 178, 2017.
- [4] Khaled Q. Abdelfadeel, Victor Cionca, and Dirk Pesch. A fair adaptive data rate algorithm for lorawan. 2018.
- [5] F. Adelantado, X. Vilajosana, P. Tuset-Peiro, B. Martinez, J. Melia-Segui, and T. Watteyne. Understanding the limits of lorawan. *IEEE Communications Magazine*, 55(9):34–40, 2017.
- [6] Aloys Augustin, Jiazi Yi, Thomas Clausen, and William Mark Townsley. A study of lora: Long range & low power networks for the internet of things. *Sensors*, 16(9), 2016.
- [7] D. Bankov, E. Khorov, and A. Lyakhov. Mathematical model of lorawan channel access. In *2017 IEEE 18th International Symposium on A World of Wireless, Mobile and Multimedia Networks (WoWMoM)*, pages 1–3, June 2017.
- [8] Martin Bor, John Vidler, and Utz Roedig. Lora for the internet of things. In *Proceedings of the 2016 International Conference on Embedded Wireless Systems and Networks, EWSN '16*, pages 361–366, 2016.
- [9] Lluís Casals, Bernat Mir, Rafael Vidal Ferré, and Carles Gomez. Modeling the energy performance of lorawan. In *Sensors*, 2017.
- [10] Marco Cattani, Carlo Alberto Boano, and Kay Rmer. An experimental evaluation of the reliability of lora long-range low-power wireless communication. *Journal of Sensor and Actuator Networks*, 6(2), 2017.
- [11] Semtech Corporation. Reading channel rssi during a cad. <https://loro-developers.semtech.com/library/product-documents/>.
- [12] Francesca Cuomo, Manuel Campo, Alberto Caponi, Giuseppe Bianchi, and Patrizio Pisani. Explora: Extending the performance of lora by suitable spreading factor allocations. In *IEEE International Conference on Wireless & Mobile Computing*, 2017.
- [13] A. Dongare, C. Hesling, K. Bhatia, A. Balanuta, R. L. Pereira, B. Iannucci, and A. Rowe. Openchirp: A low-power wide-area networking architecture. In *2017 IEEE International Conference on Pervasive Computing and Communications Workshops (PerCom Workshops)*, pages 569–574, March 2017.
- [14] Wan Du, Jansen Christian Liando, Huanle Zhang, and Mo Li. When pipelines meet fountain: Fast data dissemination in wireless sensor networks. In *Proceedings of the 13th ACM Conference on Embedded Networked Sensor Systems*, pages 365–378, 2015.
- [15] Rashad Eletreby, Diana Zhang, Swarn Kumar, and Osman Yağan. Empowering low-power wide area networks in urban settings. *SIGCOMM '17*, pages 309–321, 2017.
- [16] T. Elshabrawy and J. Robert. Closed-form approximation of lora modulation ber performance. *IEEE Communications Letters*, 2018.
- [17] B. C. Fargas and M. N. Petersen. Gps-free geolocation using lora in low-power wans. In *2017 Global Internet of Things Summit (GloTS)*, pages 1–6, June 2017.
- [18] Weifeng Gao, Wan Du, Zhiwei Zhao, Geyong Min, and Mukesh Singhal. Towards energy-fairness in lora networks. In *2019 IEEE 39th International Conference on Distributed Computing Systems (ICDCS)*, pages 788–798, 2019.
- [19] Sakshama Ghosly. All about lora and lorawan. <https://www.sghosly.com/>.
- [20] T. Hadwen, V. Smallbon, Q. Zhang, and M. D'Souza. Energy efficient lora gps tracker for dementia patients. In *2017 39th Annual International Conference of the IEEE Engineering in Medicine and Biology Society (EMBC)*, pages 771–774, July 2017.
- [21] V. Hauser and T. Hegr. Proposal of adaptive data rate algorithm for lorawan-based infrastructure. In *2017 IEEE 5th International Conference on Future Internet of Things and Cloud (FiCloud)*, volume 00, pages 85–90, Aug. 2017.
- [22] J. W. Huang, Q. Zhu, V. Krishnamurthy, and T. Basar. Distributed correlated q-learning for dynamic transmission control of sensor networks. In *2010 IEEE International Conference on Acoustics, Speech and Signal Processing*, 2010.
- [23] LoRa Alliance Inc. <https://loro-alliance.org/resource-hub/lorawan-specification-v11>, 2017.
- [24] Yahya Javed, Adeel Baig, and Maajid Maqbool. Enhanced quality of service support for triple play services in ieee 802.11 wans. *Eurasip Journal on Wireless Communications & Networking*, 2015.
- [25] O. Khutsoane, B. Isong, and A. M. Abu-Mahfouz. Iot devices and applications based on lora/lorawan. In *IECON 2017 - 43rd Annual Conference of the IEEE Industrial Electronics Society*, pages 6107–6112, Oct 2017.
- [26] J. M. Marais, R. Malekian, and A. M. Abu-Mahfouz. Lora and lorawan testbeds: A review. In *2017 IEEE AFRICON*, pages 1496–1501, Sept 2017.
- [27] P. P. Priyesh and S. K. Bharti. Dynamic transmission power control in wireless sensor networks using p-i-d feedback control technique. In *2017 9th International Conference on Communication Systems and Networks (COMSNETS)*, 2017.
- [28] U. Raza, P. Kulkarni, and M. Sooriyabandara. Low power wide area networks: An overview. *IEEE Communications Surveys Tutorials*, 19(2):855–873, 2017.
- [29] Jothi Prasanna Shanmuga Sundaram, Wan Du, and Zhiwei Zhao. A survey on lora networking: Research problems, current solutions and open issues. *IEEE Communications Surveys & Tutorials*, 2019.
- [30] Jun Min Yi, Eom Ji Oh, Dong Kun Noh, and Ikjune Yoon. Energy-aware data compression and transmission range control for energy-harvesting wireless sensor networks. *International Journal of Distributed Sensor Networks*, 2017.